

High Time Resolution Monitoring of Tropospheric Temperature with a Radio Acoustic Sounding System (RASS)

T. TSUDA,¹ Y. MASUDA,² H. INUKI,² K. TAKAHASHI,² T. TAKAMI,¹ T. SATO,¹
S. FUKAO,¹ and S. KATO¹

Abstract—We have observed the time-height variation of the temperature field in the upper troposphere using a Radio Acoustic Sounding System (RASS) which consists of the MU radar and a high-power acoustic transmitter. The fast beam steerability of the MU radar has made it possible to measure temperature profiles in a fairly wide height range in the upper troposphere (5–11 km), even under intense wind conditions. Observations were continued for about 32 hr on 24–26 December, 1986 with a time-height resolution of 30 min and 150 m. During the observation period, the tropospheric jet was so intense that the acoustic wavefronts were severely distorted. Using wind velocity profiles observed by the MU radar we have numerically estimated the propagation of acoustic wavefronts, and further determined favorable pointing directions for the MU radar to receive significant backscattering from refractive index fluctuations produced by the acoustic waves. Conventional radiosonde soundings were carried out every 6 hr, which showed a temperature decrease of 4 K/day in the upper troposphere during the observation period. Temperature profiles taken by RASS agree well with the radiosonde results.

Key words: RASS, troposphere, temperature profile, MU radar, acoustic transmitter, radiosonde, remote sensing.

1. Introduction

The Radio Acoustic Sounding System (RASS) is a ground-based remote sensing technique of atmospheric temperature in the troposphere and lower stratosphere (*e.g.*, MARSHALL *et al.*, 1972). The RASS utilizes the physical principle that radar echoes are scattered from periodic fluctuations in refractive index due to the density fluctuations produced by acoustic waves.

There are two fundamental conditions to receive significant RASS echoes by using a monostatic radar. First, the radar beam must be pointed in a direction such that the beam is normal to the acoustic wavefronts so that the reflections are back to the radar antenna. MASUDA (1988) extensively studied modification of acoustic

¹ Radio Atmospheric Science Center, Kyoto University, Uji, Kyoto 611, Japan.

² Communications Research Laboratory, Ministry of Posts and Telecommunications, Koganei, Tokyo 184, Japan.

wavefronts attributed to mean vertical gradients of both temperature and wind fields, and proved the importance of this condition by investigating a two-dimensional numerical model and RASS observations with the MU radar.

Second, the refractive index fluctuation should have a scale equal to half of the radar wavelength to satisfy the Bragg condition. So that, frequencies of the transmitted acoustic waves must be appropriately tuned according to mean temperature and wind profiles.

Because intensity of the RASS echoes becomes the largest when the Bragg condition is completely satisfied, it is often assumed, for intense RASS echoes, that the Doppler frequency corresponding to the propagation speed of acoustic pulses is the same as the transmitted acoustic frequency. However, MATUURA *et al.* (1986) pointed out that the Doppler shift of RASS echoes is not necessarily equal to the transmitted acoustic frequency. In other words, the intense RASS echoes could be received even when the Bragg condition is not strictly satisfied, which seems to be attributed to a delicate balance between the first and second conditions (MATUURA *et al.*, 1986). Therefore, it is important to determine the apparent sound speed from actual measurements of Doppler shift of the RASS echoes by the radar. The apparent sound speed thus obtained as a function of height is further converted to the temperature profile after compensating the Doppler shift effect due to the radial wind velocity.

By combining the MU radar (KATO *et al.*, 1984; FUKAO *et al.*, 1985a,b) with a high-power acoustic transmitter, MATUURA *et al.* (1986) have observed the temperature profile at the altitude range of 6–22 km in August 1985. In summer, the tropospheric jet becomes relatively weak, therefore, acoustic waves stay over the MU radar even in the lower stratosphere. On the other hand, in winter the maximum speed of the jet sometimes exceeds 100 m/s, thus, it becomes difficult to measure the temperature profile above the tropopause. In this paper, we report continuous monitoring of the tropospheric temperature profile using the RASS with the MU radar on 24–26 December, 1986. During the observation period the jet was fairly intense, so that the height range was limited to the 5–11 km altitude range.

2. Experimental Setup and Data Analysis

The RASS used in this paper consists of a high-power acoustic transmitter (MATUURA *et al.*, 1986) and the MU radar with a radio wavelength of 6.45 m which is described in detail elsewhere (KATO *et al.*, 1984; FUKAO *et al.*, 1985a,b). Figure 1 shows a block diagram of the acoustic transmitter. High pressure air flow with around 7 atm of pressure is gated by an electromagnetic valve. Sinusoidal acoustic waves are produced by modulating the pulsed air flow by a pneumatic transducer, and further transmitted upward from a hyperbolic horn with a diameter of 72 cm which is efficient in a frequency band of 77–110 Hz. The double side beam

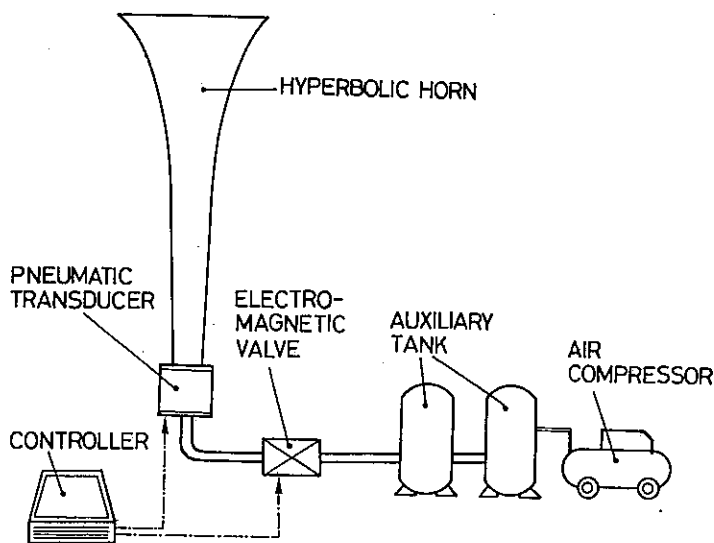


Figure 1
A block diagram of the acoustic transmitter.

width of the horn is approximately 100° . The sound pressure level of the acoustic wave 1 m above the horn is 500 W/m^2 . The pulse repetition frequency and duration of the acoustic pulse, as well as the acoustic frequency, are controlled by a system-installed small computer.

MASUDA (1988) found that the height range of the RASS measurement is mainly determined by vertical gradients of background temperature and mean winds, and is also a strong function of distance between sound and radar antennas. We have regularly observed vertical, northward and eastward components of wind velocity by the MU radar, and temperature profiles using conventional radiosondes before and during the RASS observations.

A two-dimensional ray tracing of the acoustic waves, which is described by MASUDA (1988) in detail, is applied to estimate the shape of the wavefronts and the effective reflection region of the RASS echoes. Figure 2 shows typical profiles of temperature and eastward radial winds measured by a radiosonde and the MU radar. The radial wind velocity shown in Figure 2 was sampled at a zenith angle of 10° , therefore, the corresponding maximum horizontal wind velocity at around 11 km altitude was as large as 90 m/s. This wind profile is approximated by linear sections in several altitude regions for the numerical computations of the acoustic ray-tracing (MASUDA, 1988). Two reflection regions appear in the windward and leeward directions at zenith angles of around 30° and 50° , respectively, as shown in Figure 2. The former direction is preferable for the MU radar observations. The initial numerical ray-tracing of acoustic waves was done in advance of the continuous RASS observation. By taking the results into account, the acoustic transmitter

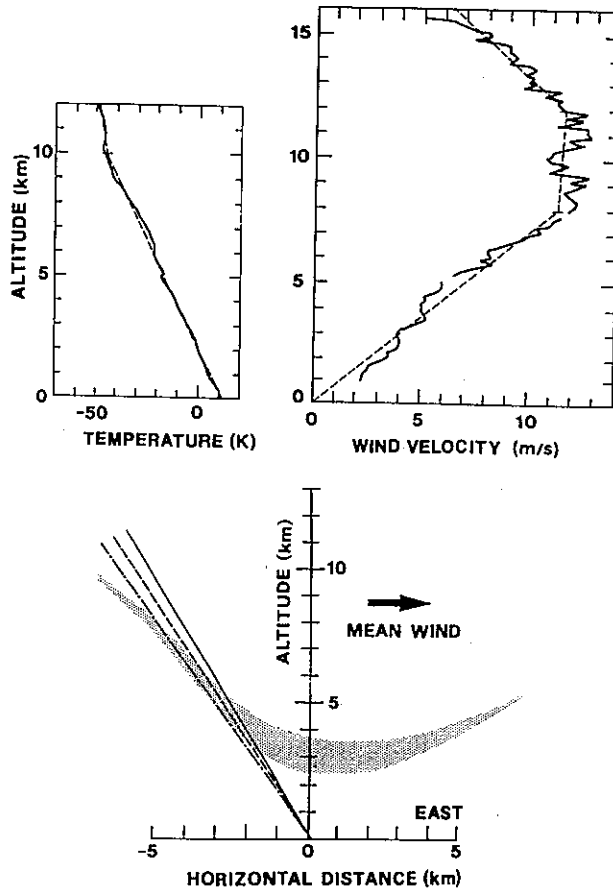


Figure 2

Temperature (top left) and eastward radial wind velocity (top right) profiles measured by a radiosonde and the MU radar, respectively, at around 11:30 on Dec. 25, and a two-dimensional numerical model of the effective reflection region of RASS echoes (bottom). The distance between the sound and radar antennas is assumed to be 120 m.

was located 120 m west of the center of the MU radar antenna, because the mean winds were nearly in the eastward direction. The ray-tracing was continued during the observations in order to determine suitable beam directions on a real-time basis. In general, time variation of the gradient and direction of mean winds is larger than that of the temperature gradient, therefore, the mean wind structure should be more frequently monitored than the temperature profile.

In the actual observations, several beam directions are necessary to cover the large height range, and follow small-scale excursions of the reflection regions from the directions which were deduced from the numerical model. Since the MU radar can change the azimuth and zenith angles of the antenna beam every 5° and $1\text{--}2^\circ$,

respectively, we have steered the radar beam in four directions as listed in Table 1. Because the meridional component of the mean wind varied slightly with time, we have steered the antenna beam towards the north or south from the westward direction. We did not move the acoustic transmitter throughout the RASS observations. However, it might become necessary to relocate the acoustic transmitter such that it is placed in the windward direction from the center of the radar antenna, when the meridional wind varies largely from the initial condition.

As shown in Figure 3, we have transmitted two sets of eight successive acoustic pulses with a pulse width of approximately 0.5 sec and an interval of 2 sec. Each pulse contained 50 cycles of acoustic waves. Because of the mean temperature decrease in the troposphere, the acoustic frequency suitable for the Bragg condition decreases with height. Therefore, the frequency was changed from 88 to 95 Hz and from 81–88 Hz for temperature soundings in the lower and upper height ranges, respectively, as shown in Figure 3.

The transmitted radar pulse was phase-modulated by a 16-bit complementary code with a subpulse width of 1 μ sec. The RASS echoes were sampled with a range resolution of 150 m, and transferred into Doppler spectra using a 1024-point FFT. The number of coherent integration is limited to two in each antenna direction, giving an effective sampling rate of 3.2 msec in order to cover a wide Doppler velocity range corresponding to the sound speed of around 300 m/s. The total height range was separated into two regions consisting of 32 altitude points, because of restrictions of the memory area for Doppler spectra in the MU radar.

Although the RASS observations can be finished in a few min as recognized from Figure 3, they are repeated every 30 min, with the repetition frequency mainly limited by the refilling time of the high-pressure tanks by the air compressor. The three components of the wind field are observed by the MU radar using a normal MST radar technique during the observation gaps of two successive RASS measurements.

An apparent sound speed is determined at each range gate by applying a least-square fitting of a Gaussian to the Doppler spectra of the RASS echoes. By

Table 1

Antenna beam directions of the MU radar during the RASS observations.

Observation Period	[Azimuth angle, Zenith angle (°)]
16:00 Dec. 24 – 8:30 Dec. 25	[270, 30], [275, 28], [275, 30], [275, 32]
8:30 Dec. 25 – 13:00 Dec. 25	[260, 30], [265, 28], [265, 30], [265, 32]
13:00 Dec. 25. – 17:30 Dec. 25	[260, 30], [260, 32], [260, 34], [265, 32]
17:30 Dec. 25 – 00:00 Dec. 26	[260, 32], [265, 32], [265, 34], [270, 32]

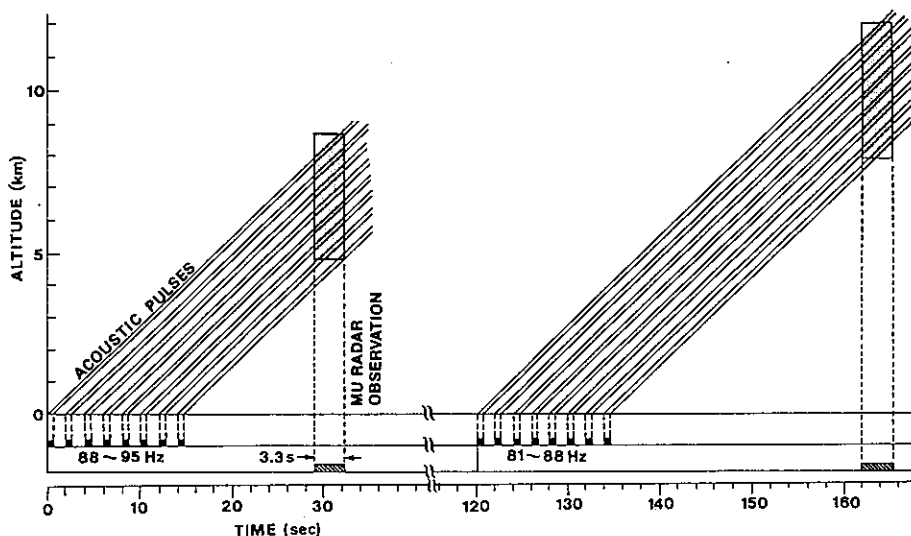


Figure 3

A timing chart of the acoustic pulses and the MU radar observations. Eight successive pulses with width and repetition period of 0.5 and 2 sec, respectively, are transmitted twice for the RASS observations of lower (5–9 km) and upper (8–12 km) altitudes. The RASS echoes are sampled by the MU radar 29 and 42 sec after the transmission of acoustic pulses.

linearly interpolating the wind fields detected before and after the RASS observations, we can re-compose the radial wind velocity in the antenna beam direction for the RASS measurements. A true sound speed, C (ms^{-1}) is determined after compensating this radial wind velocity from the apparent sound speed, and further transferred into the atmospheric temperature T ($^{\circ}\text{K}$) by utilizing a relation of $C = 20.067T^{0.5}$. Temperature profiles independently determined in four beam directions are projected onto a single altitude axis with a step of 100 m after interpolation. These temperature profiles are further smoothed by applying a moving average of five adjacent altitude points with a triangular weighting. A representative value of the atmospheric temperature is determined, when the discrepancy among the four different determinations is small. Thus, temperature profiles with a time resolution of 30 min are found from the RASS observations. We have further averaged over three profiles, again using a triangular weighting when these are compared with the radiosonde measurements.

3. Results and Discussions

Figure 4 shows the eastward and northward components of the mean wind velocity observed by the MU radar in a period from 16:00, Dec. 24 to 00:00 Dec. 26, 1986, and atmospheric temperature profiles averaged over five radiosonde

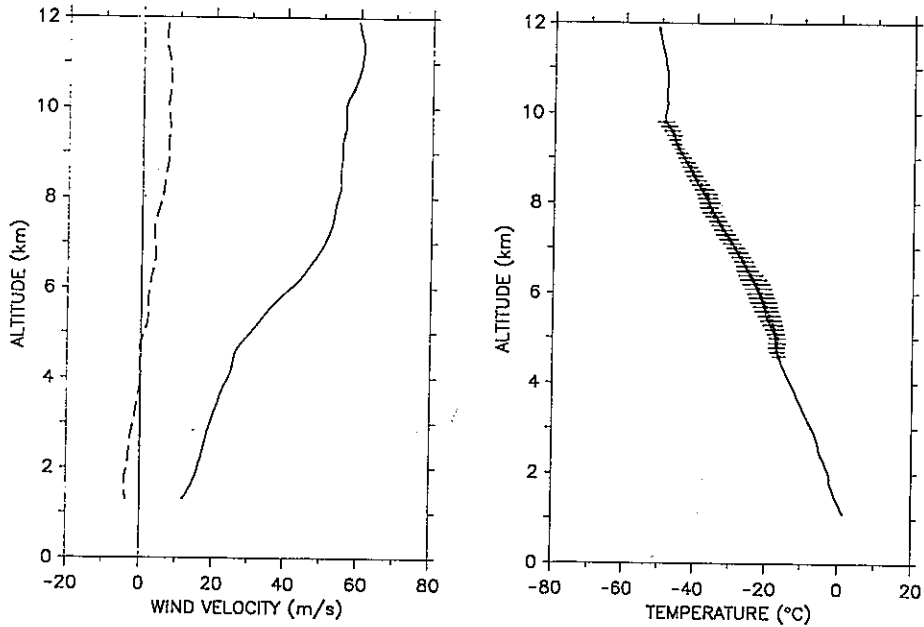


Figure 4

Eastward (solid line) and northward components (broken line) of the mean horizontal winds observed by the MU radar in a period from 16:00, Dec. 24 to 00:00 Dec. 26, 1986 (left panel), and atmospheric temperature profiles (solid line) averaged over five radiosonde measurements which were made every 6 hr starting from 23:00, Dec. 24 at the MU radar site (right panel). The latter is compared with a mean temperature profile averaged over 24 hr of RASS observations (circle) made on 24–26 December, 1986. Error bar corresponds to standard deviation of temperature fluctuations during the observation period.

measurements made every 6 hr starting from 23:00, Dec. 24 at the MU radar site. The latter is compared with a mean temperature profile from the RASS measurements averaged over 24 hr corresponding to the entire observation period of radiosonde soundings. The tropospheric wind is nearly eastward in the whole height range, and its maximum exceeds 60 ms^{-1} at around 11 km. The meridional wind becomes slightly northward above 5 km. Agreement of the temperature profiles is excellent, although the standard deviation around the mean value becomes large at around 6 km altitude, which may be attributed to a rapid change in the temperature fields as described later.

Figure 5 shows relatively large fluctuations in the temperature profiles in the troposphere from radiosonde observations made every 6 hr from 23:00 Dec. 24 to 23:00 Dec. 25, 1986. The temperature below 10 km altitude decreases by 5–10 K in 24 hr, which is most clearly seen at around 5 km altitude, while it generally increases in the altitude region above 10 km.

Individual temperature profiles taken by the radiosondes plotted in Figure 5, are reproduced in Figure 6 with successive soundings shifted by 72 K, and are

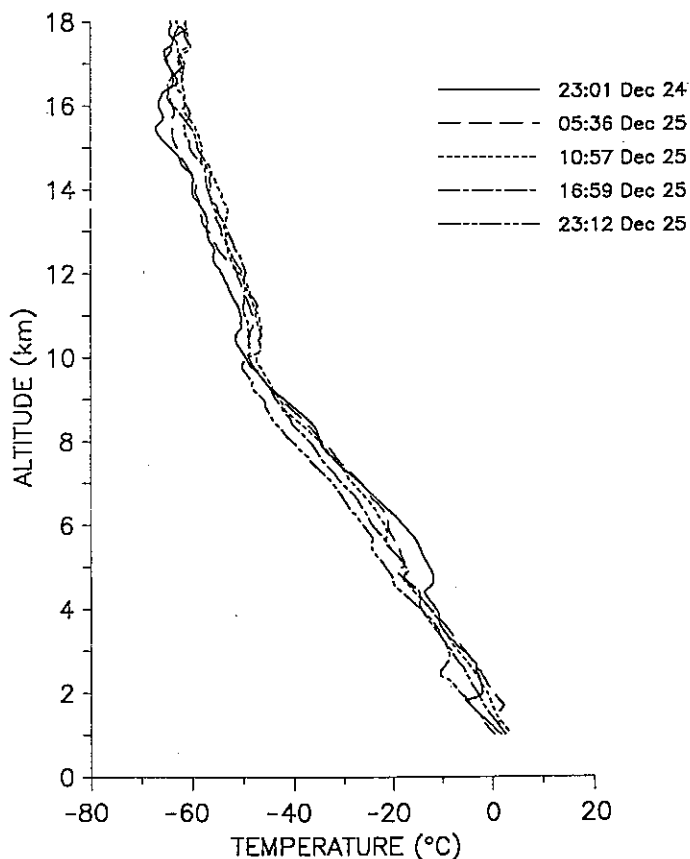


Figure 5
Temperature profiles observed by five radiosondes.

compared with RASS observations. Although there exists a general temperature decrease in the observed height range as shown in Figure 5, temperature profiles from RASS measurements agree fairly well with the conventional radiosonde results. Furthermore, the phase progression of wave-like structure can be recognized from RASS observations at 5–7 km in the first third of the observation period.

Figure 7 shows contour plots of the tropospheric temperature from radiosonde and RASS observations. Because there are only five profiles from radiosonde measurements, the time variation in the upper panel looks fairly smooth. Isotherms in the 7–9.5 km altitudes generally stay at the same height until 12:00 Dec. 25, then linearly decrease at an approximate rate of 60 m/hr. The altitude of the -15°C isotherm drastically falls during the first four hr. The 20°C isotherm starting at an altitude of 6.2 km at 23:00 on Dec. 24 also descends by about 1 km during the first ten hr, and then does not vary largely in the middle of the observation

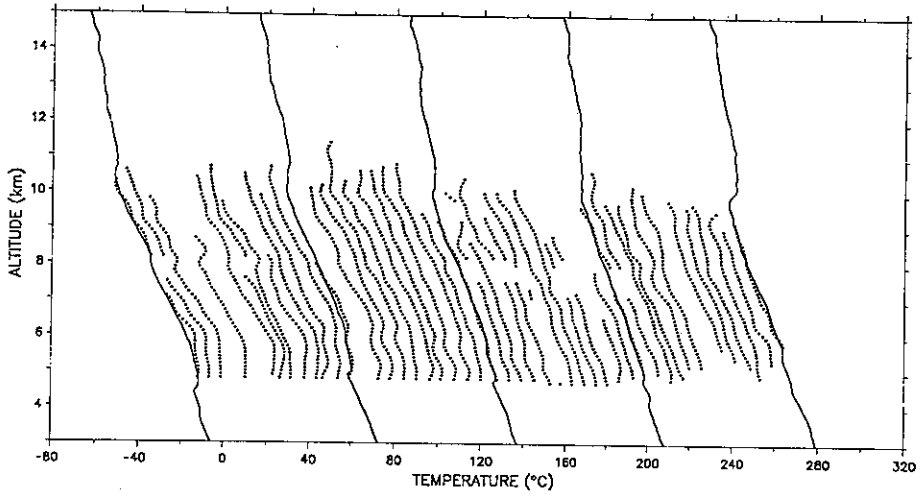


Figure-6

Temperature profiles taken every 30 min by RASS (dots) and radiosondes (solid lines). Horizontal axis is shifted by 6 and 72 K for every temperature profile determined by RASS and radiosonde measurements, respectively.

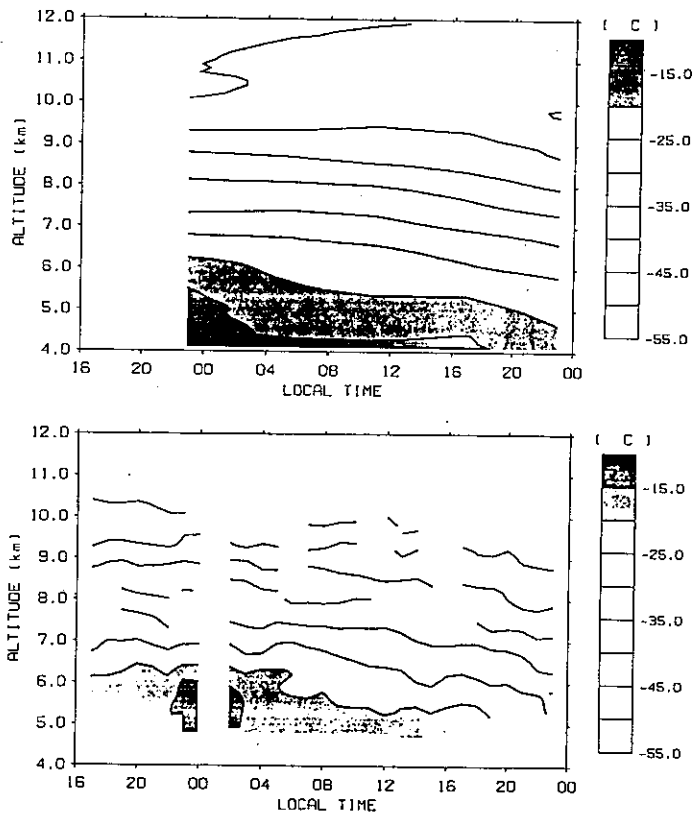


Figure 7

Contour plots of the tropospheric temperature by radiosondes (top) and RASS (bottom).

period. This isotherm then falls linearly during the latter part of the observation period.

The RASS observations show overall agreement with the radiosonde results and furthermore, they exhibit fine structure of temperature fluctuations in addition to the general trends. For an example, we can recognize a core of local high temperature centered at 5.5 km altitude and 01:00 on Dec. 25. In general, RASS is a powerful tool to investigate meso-scale fluctuations in temperature fields with relatively good time and height resolution.

4. Concluding Remarks

In this paper, we have presented RASS measurements of atmospheric temperature in the upper troposphere (5–11 km) made every 30 min for 32 hr on 24–26 Dec., 1986. The mean temperature profiles, averaged over 24 hr of RASS measurements, agree very well with the conventional radiosonde observations. Individual temperature profiles taken by the radiosonde are fairly well reproduced by the RASS measurements, even though there was a large decrease of background temperature during the observation period.

The sampling interval of temperature profiles is mainly determined by the recovery time of the air pressure in the tank and therefore by the refilling capacity of the compressing system. The time resolution can be fairly easily improved up to several minutes by improving the air compressor installed on the acoustic transmitter. When the mean wind is relatively weak, acoustic wavefronts are not severely modified, and the effective reflection regions of RASS echoes do not move windward, but stay near the acoustic transmitter even at an altitude of 25 km (MATUURA *et al.*, 1985; MASUDA, 1988). In such a condition, we would be able to continuously monitor variation of lower stratospheric temperature with a time-height resolution of several min and a few hundred m. If the fine structure of temperature fields are observed by using the RASS technique in addition to precise measurements of wind velocities by the MST radars, we will acquire a new perspective on meso- and micro-scale fluctuations in the troposphere and lower stratosphere.

Acknowledgements

Helpful suggestions by Drs. T. E. VanZandt, P. T. May and R. J. Doviak are warmly acknowledged. Data used in this paper were obtained by using a pneumatic transducer borrowed from Ship Research Institute, Japanese Ministry of Transport. The MU radar is operated by the Radio Atmospheric Science Center, Kyoto University.

REFERENCES

- FUKAO, S., T. SATO, T. TSUDA, S. KATO, K. WAKASUGI, and T. MAKIHIRA (1985a), *The MU radar with an active phased array system: 1. Antenna and power amplifiers*, Radio Sci. 20, 1155-1168.
- FUKAO, S., T. TSUDA, T. SATO, S. KATO, K. WAKASUGI, and T. MAKIHIRA (1985b), *The MU radar with an active phased array system: 2. In-house equipment*, Radio Sci. 20, 1169-1176.
- KATO, S., T. OGAWA, T. TSUDA, T. SATO, I. KIMURA, and S. FUKAO (1984), *The middle and upper atmosphere radar: First results using a partial system*, Radio Sci. 19, 1475-1484.
- MARSHALL, J. M., A. M. PETERSON, and A. A. BARNES, Jr. (1972), *Combined Radar-Acoustic Sounding System*, Appl. Optics 11, 108-112.
- MASUDA, Y. (1988), *The dependence of altitude limit of Radio Acoustic Sounding System (RASS) upon wind and temperature gradients*, Radio Sci. 23, 647-654.
- MATUURA, N., Y. MASUDA, H. INUKI, S. KATO, S. FUKAO, T. SATO, and T. TSUDA (1986), *Radio acoustic measurement of temperature profile in the troposphere and stratosphere*, Nature 323, 426-428.

(Received September 14, 1987, revised/accepted February 18, 1988)